

# $CP$ violation and material interaction of neutral kaons in measurements of the CKM angle $\gamma$ using $B^\pm \rightarrow DK^\pm$ decays where $D \rightarrow K_S^0 \pi^+ \pi^-$

---

M. Bjørn and S. Malde,

*University of Oxford,  
Oxford,  
United Kingdom*

*E-mail:* [mikkel.bjoern@physics.ox.ac.uk](mailto:mikkel.bjoern@physics.ox.ac.uk), [sneha.malde@physics.ox.ac.uk](mailto:sneha.malde@physics.ox.ac.uk)

ABSTRACT:

As measurements of the CKM angle  $\gamma$  in decays of  $b$ -hadrons become increasingly precise, it is important to consider the impact of processes that affect secondary and tertiary decay products and can contribute to the observed  $CP$  violation. The golden decay mode used to measure  $\gamma$  is  $B \rightarrow DK$ , where  $D \rightarrow K_S^0 \pi^+ \pi^-$ . Due to the presence of a  $K_S^0$  meson in the final state,  $\gamma$  measurements based on this mode are affected by neutral kaon  $CP$  violation and matter regeneration, and this study examines the potential size of the impact. Previous studies determine the impact of kaon  $CP$  violation to be a few degrees in size, but make simplifying assumptions about how experimental measurements are implemented. These assumptions are lifted in the present study, and the matter regeneration effect is included for the first time. The results are presented within the context of  $\gamma$  measurements to be made using the LHCb and Belle II detectors. It is found that the expected biases due to ignoring the effects of  $CP$  violation and matter regeneration in neutral kaons is small and less than  $0.5^\circ$  degrees in all experimental scenarios considered.

## 1 Introduction

The  $CP$ -violating phase  $\gamma \equiv \arg(-V_{ud}V_{ub}^*/V_{cd}V_{cb}^*)$  of the Cabibbo-Kobayashi-Maskawa (CKM) matrix [1, 2] in the Standard Model (SM) is the only CKM angle that can easily be measured via tree-level processes. It therefore provides an important SM benchmark measurement that can be compared with estimates based on other CKM observables, more likely to be affected by new physics effects [3]. Interference between  $B \rightarrow D^0 K$  and  $B \rightarrow \bar{D}^0 K$  decay amplitudes provide an important way to measure  $\gamma$ . Measurements have been made in a range of  $B \rightarrow DK$  modes [4–7], which are combined to provide the best estimate of  $\gamma$  from direct measurements, with a current uncertainty of about  $5^\circ$  [6–8].

An important contribution comes from  $B^\pm \rightarrow DK^\pm$  decays in which  $D \rightarrow K_S^0 \pi^+ \pi^-$ , where  $D$  describes a superposition of  $D^0$  and  $\bar{D}^0$  states. In this decay,  $\gamma$  can be determined by analysing the phase-space distribution of the  $D$  decay, as proposed in Refs. [9–11] and [12]. This approach has been used to measure  $\gamma$  by the Belle [13–16], BaBar [17–19], and LHCb collaborations [20–24], with the latest measurement from LHCb [24] constituting the most precise stand-alone  $\gamma$  measurement to date. The LHCb and Belle II collaborations both expect to reach a precision of at least  $\sigma(\gamma) \lesssim 3^\circ$  in measurements that use the method during the coming decade, with LHCb expecting a statistical uncertainty below  $1^\circ$  in its proposed Upgrade II phase [25, 26].

However, the presence of a  $K_S^0$  meson in the final state constitutes an additional source of  $CP$  violation in  $B^\pm \rightarrow D(\rightarrow K_S^0 \pi^+ \pi^-)K^\pm$  decays, due to  $CP$  violation in the neutral kaon system. The effect has been broadly ignored experimentally, as the statistical uncertainty has so far been much larger than the expected induced bias on the measured value of  $\gamma$ . Previous studies have estimated this bias to be up to a few degrees [27]. In Ref. [27], the estimates are based on phase-space-integrated yield asymmetries, however the current experimental approach is based on  $CP$  asymmetries within the phase-space distribution of signal decays. This paper focuses on the latter approach, and removes some of the assumptions made in Ref. [27]. Furthermore, material interaction of the neutral kaon in the detector can lead to experimental signatures that mimic those of  $CP$  violation, and thus introduce an additional source of measured  $CP$  asymmetry, which can be of a similar size to the asymmetry from inherent  $CP$  violation in the neutral kaon system [28, 29]. Therefore, a detailed understanding of both effects will be necessary as the statistical uncertainties on  $\gamma$  measurements based on  $B^\pm \rightarrow D(\rightarrow K_S^0 \pi^+ \pi^-)K^\pm$  decays enter the few degree range.

## 2 Measurements of $\gamma$ using $B^\pm \rightarrow D(\rightarrow K_S^0 \pi^+ \pi^-)K^\pm$ decays

This section introduces the theory of  $\gamma$  measurements based on  $B^\pm \rightarrow D(\rightarrow K_S^0 \pi^+ \pi^-)K^\pm$  decays and the current experimental practice in Section 2.1, then describes the effects of neutral kaon  $CP$  violation and material interaction in Section 2.2, and gives an estimate of the expected impact on experimental results in Section 2.3.

### 2.1 Theory and current experimental practice

The amplitude for the decay  $B^- \rightarrow D(\rightarrow K_S^0(\rightarrow \pi^+ \pi^-)\pi^+ \pi^-)K^-$ , denoted  $\mathcal{A}_S^-$ , can be written as a superposition of the amplitude for a  $B^- \rightarrow D^0 K^-$  decay and the suppressed

$B^- \rightarrow \bar{D}^0 K^-$  decay

$$\mathcal{A}_S^-(s_-, s_+) = A_B A_{K_S^0} \left( A_S^D(s_-, s_+) + r_B \exp[i(\delta_B - \gamma)] A_S^{\bar{D}}(s_-, s_+) \right), \quad (2.1)$$

where  $r_B$  is the ratio of the magnitudes of the  $B^- \rightarrow \bar{D}^0 K^-$  and  $B^- \rightarrow D^0 K^-$  amplitudes,  $\delta_B$  is the strong phase between them,  $A_B$  is the amplitude of the  $B^- \rightarrow D^0 K^-$  decay,  $A_{K_S^0}$  is the amplitude of the  $K_S^0 \rightarrow \pi^+ \pi^-$  decay,  $s_-$  and  $s_+$  are the squared invariant masses of the  $K_S^0 \pi^-$  and  $K_S^0 \pi^+$  particle combinations, respectively, and the  $D$  decay amplitudes are defined as

$$A_{S(L)}^{\bar{D}}(s_-, s_+) = A(\bar{D}^0 \rightarrow K_{S(L)}^0 \pi^+ \pi^-). \quad (2.2)$$

Biases from the effects of  $D^0 - \bar{D}^0$  mixing are potentially significant, but can be confined to  $0.1^\circ$  with an appropriate measurement strategy. These effects are described in Ref. [30] and are not discussed further in this study. Direct  $CP$  violation in the  $D$  decay is assumed to be negligible, as the effect is expected to be very small for  $D \rightarrow K_S^0 \pi^+ \pi^-$  decays in the SM, and has been analysed in Ref. [31]. Under the further assumption that  $K_S^0$  is a  $CP$  eigenstate, the  $D$  decay amplitudes satisfy

$$A_S^{\bar{D}}(s_{-+}) = A_S^D(s_{+-}), \quad (2.3)$$

where the short-hand notation  $(s_{-+}) = (s_-, s_+)$  and  $(s_{+-}) = (s_+, s_-)$  is employed to simplify equations. The differential  $B^- \rightarrow D(\rightarrow K_S^0 \pi^+ \pi^-) K^-$  decay rate to a given point in the  $D$  decay phase space is

$$d\Gamma^-(s_{-+}) \propto |\mathcal{A}_S^-|^2 = |A_B|^2 |A_{K_S^0}|^2 \left[ |A_S^D(s_{-+})|^2 + r_B^2 |A_S^D(s_{+-})|^2 + 2r_B |A_S^D(s_{-+})| |A_S^D(s_{+-})| \times (\cos[-\Delta\delta_D(s_{-+})] \cos[\delta_B - \gamma] - \sin[-\Delta\delta_D(s_{-+})] \sin[\delta_B - \gamma]) \right]. \quad (2.4)$$

Here,  $\Delta\delta_D(s_{-+}) = \delta_D(s_{-+}) - \delta_D(s_{+-})$ , where  $\delta_D(s_{-+})$  denotes the phase of  $A_S^D(s_{-+})$ . The equivalent expressions to Eq. (2.1) and Eq. (2.4) for  $B^+ \rightarrow D(\rightarrow K_S^0 \pi^+ \pi^-) K^+$  decays are obtained via the substitutions  $\gamma \rightarrow -\gamma$  and  $A_S^D(s_{-+}) \leftrightarrow A_S^{\bar{D}}(s_{-+})$ , where the latter substitution is equivalent to  $A_S^D(s_{-+}) \leftrightarrow A_S^D(s_{+-})$ .

Based on Eq. (2.4), it is possible to measure  $\gamma$  (and the nuisance parameters  $r_B$  and  $\delta_B$ ) from the phase-space distribution of  $B^\pm \rightarrow D(\rightarrow K_S^0 \pi^+ \pi^-) K^\pm$  decays, given knowledge of  $\delta_D(s_{-+})$  or  $\Delta\delta_D(s_{-+})$ . A series of  $\gamma$  measurements have used amplitude models of the  $D$  decay to describe  $\Delta\delta_D(s_{-+})$  [14–21]. More recently, a model-independent approach, which is critical when looking for evidence of beyond-the-SM effects [13, 22–24], has been favoured. The  $D$  decay phase space is split into  $2 \times N$  regions, or bins, numbered  $i = -N$  to  $N$  (omitting zero) that are defined to be symmetric around  $s_- = s_+$ , with  $i > 0$  for  $s_- > s_+$ . The binning scheme used in current experimental measurements of  $B^\pm \rightarrow DK^\pm$  decays [13, 22, 24] has  $N = 8$  and is shown in Fig. 1. Then, the average of  $\cos \Delta\delta_D(s_{-+})$  over bin  $i$  of the  $D$  decay phase space is

$$c_i = \frac{\int_i ds^2 |A_S^D(s_{-+})| |A_S^D(s_{+-})| \cos[\Delta\delta_D(s_{-+})]}{\sqrt{\int_i ds^2 |A_S^D(s_{-+})|^2} \sqrt{\int_i ds^2 |A_S^D(s_{+-})|^2}}, \quad (2.5)$$

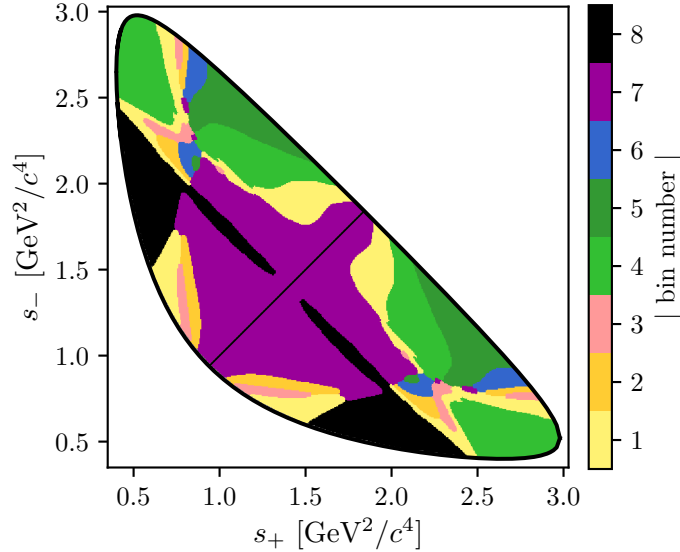


**Figure 1:** The *optimal binning scheme* of the  $D \rightarrow K_s^0 \pi^+ \pi^-$  phase space [32].

where  $\int_i ds^2$  denotes integration over bin  $i$  of the  $D$  decay phase space, and with an analogous definition of  $s_i$ , the average of  $\sin \Delta \delta_D(s_{-+})$ . Integrating Eq. (2.4), and the corresponding expression for  $B^+ \rightarrow DK^+$  decays, the yields of  $B^\pm \rightarrow D(\rightarrow K_s^0 \pi^+ \pi^-)K^\pm$  in bin  $i$  are

$$\begin{aligned} N_i^- &= h_B^- \left( K_i + r_B^2 K_{-i} + 2\sqrt{K_i K_{-i}} (c_i x_- + s_i y_-) \right), \\ N_i^+ &= h_B^+ \left( K_{-i} + r_B^2 K_i + 2\sqrt{K_i K_{-i}} (c_i x_+ - s_i y_+) \right), \end{aligned} \quad (2.6)$$

in terms of the integrals

$$K_i = \frac{1}{N_K} \int_i ds^2 |A_S^D(s_{-+})|^2, \quad N_K = \int ds^2 |A_S^D(s_{-+})|^2, \quad (2.7)$$

the normalisation constants  $h_B^\pm$ , and the  $CP$  violation observables  $x_\pm = r_B \cos(\delta_B \pm \gamma)$  and  $y_\pm = r_B \sin(\delta_B \pm \gamma)$ .

In model-independent experimental measurements of  $\gamma$ , the signal decay yields in each phase-space bin are expressed via Eq. (2.6) and  $x_\pm$  and  $y_\pm$  are determined via a maximum likelihood fit to the data. As Eq. (2.6) leads to 32 observable yields but 36 unknown parameters, it is necessary to use some external information. It is possible to measure  $c_i$  and  $s_i$  using quantum correlated  $D^0 \bar{D}^0$  pairs produced at the  $\psi(3770)$  resonance [10, 11]. Such measurements have been made by the CLEO collaboration [32], and these have been employed in a range of  $\gamma$  measurements [13, 22–24]. More precise measurements of  $c_i$  and  $s_i$  are expected from the BESIII collaboration, and further measurements could also be made from an analysis of charm mixing [33], or from reconstructed decays of the  $\psi(3770)$

meson at LHCb [34]. The  $K_i$  parameters can also be measured in external samples. It is advantageous to determine the  $K_i$  parameters from a sample that has as similar kinematics to the  $B^\pm \rightarrow DK^\pm$  sample as possible, in order to automatically include corrections from experimental effects, such as reconstruction efficiency and resolution. A sample of flavour-tagged  $D$  decays is commonly used. Given the current yields of  $B$  decays, both the strong phase and  $K_i$  parameters are taken from external input in order to maximise the sensitivity to  $x_\pm$  and  $y_\pm$ .

The interference in  $B^\pm \rightarrow D(\rightarrow K_S^0 \pi^+ \pi^-) K^\pm$  decays presents itself primarily in different distributions over the  $D$ -decay phase space between signal decays originating from  $B^+$  and  $B^-$  mesons. From an experimental point of view this is highly desirable, as production and detection asymmetries that affect the phase-space-integrated yields can be ignored. In addition to the asymmetry in the distribution over the phase space there is a further  $CP$  asymmetry in the phase-space-integrated yields, expected to be around 1%. This  $CP$  asymmetry is very challenging to measure with useful precision, due to the limited sample sizes currently available and possible biases of a similar magnitude from production and detection asymmetries. Hence, in most studies it is ignored and makes no contribution to the overall determination of  $\gamma$ .

## 2.2 $CP$ violation and material interaction of neutral kaons

The derivation in the preceding section assumed that  $K_S^0$  is a  $CP$  eigenstate, however this is known to be an approximation. Including  $CP$  violation in the neutral kaons, the mass eigenstates  $K_S^0$  and  $K_L^0$  are given by

$$|K_S^0\rangle = \frac{1}{\sqrt{1+|\epsilon|^2}} [|K_1\rangle + \epsilon|K_2\rangle], \quad |K_L^0\rangle = \frac{1}{\sqrt{1+|\epsilon|^2}} [|K_2\rangle + \epsilon|K_1\rangle], \quad (2.8)$$

in terms of the  $CP$  even (odd) eigenstates  $K_{1(2)} = (K^0 + (-)\bar{K}^0)/\sqrt{2}$  and the  $CP$  violation parameter  $\epsilon = A(K_L^0 \rightarrow \pi^+ \pi^-)/A(K_S^0 \rightarrow \pi^+ \pi^-)$ , measured to be [35]

$$|\epsilon| = (2.228 \pm 0.011) \times 10^{-3}, \quad \arg \epsilon = (43.52 \pm 0.05)^\circ. \quad (2.9)$$

The phase-convention  $\hat{C}\hat{P}|K^0\rangle = |\bar{K}^0\rangle$  is used and direct  $CP$  violation in the kaon decay is ignored, as the effect is three orders of magnitude smaller than indirect  $CP$  violation [35]. The non-zero amplitude for the  $K_L^0 \rightarrow \pi^+ \pi^-$  decay introduces a direct dependence on the  $A_L^{\bar{D}}$  amplitudes. Whereas Eq. (2.4) assumed that  $d\Gamma^-(t, s_{-+}) \propto |\psi_S^-(t, s_{-+})|^2$ , the actual decay rate satisfies

$$d\Gamma^-(t, s_{-+}) \propto |\psi_S^-(t, s_{-+}) + \epsilon\psi_L^-(t, s_{-+})|^2, \quad (2.10)$$

where  $\psi_S^-$  and  $\psi_L^-$  are the  $K_S^0$  and  $K_L^0$  components of the neutral kaon state.<sup>1</sup> The  $A_L^{\bar{D}}$  amplitudes do not satisfy Eq. (2.3), but instead  $A_L^{\bar{D}}(s_{-+}) \simeq -A_L^{\bar{D}}(s_{+-})$ , and therefore the presence of the  $K_L^0$  term leads to corrections to the yield expressions in Eq. (2.6). In

<sup>1</sup>The time dependence of Eq. (2.10) is kept implicit in Eq. (2.4), as it contributes a factor that is constant over phase-space in the  $\epsilon = 0$  approximation.

an experimental setting, the dependence on the  $A_L^{\bar{D}}$  amplitudes is further enhanced by material interactions of the neutral kaon, because different nuclear interaction strengths of the  $K^0$  and  $\bar{K}^0$  mesons introduce a non-zero  $K_S^0 \leftrightarrow K_L^0$  transition amplitude for neutral kaons traversing a detector segment. This effect was predicted early in the history of kaon physics [36] and is commonly denoted *kaon regeneration*. The general expression for the time dependent neutral kaon state components is [37, 38]

$$\begin{aligned}\psi_S(t, s_{-+}) &= e^{-i\Sigma t} \left( \psi_S^0(s_{-+}) \cos \Omega t + \frac{i}{2\Omega} (\Delta\lambda\psi_S^0(s_{-+}) - \Delta\chi\psi_L^0(s_{-+})) \sin \Omega t \right), \\ \psi_L(t, s_{-+}) &= e^{-i\Sigma t} \left( \psi_L^0(s_{-+}) \cos \Omega t - \frac{i}{2\Omega} (\Delta\lambda\psi_L^0(s_{-+}) + \Delta\chi\psi_S^0(s_{-+})) \sin \Omega t \right),\end{aligned}\quad (2.11)$$

in terms of the parameters

$$\begin{aligned}\Delta\chi &= \chi - \bar{\chi}, \\ \Delta\lambda &= \lambda_L - \lambda_S = (m_L - m_S) - \frac{i}{2}(\Gamma_L - \Gamma_S), \\ \Sigma &= \frac{1}{2}(\lambda_S + \lambda_L + \chi + \bar{\chi}), \\ \Omega &= \frac{1}{2}\sqrt{\Delta\lambda^2 + \Delta\chi^2},\end{aligned}\quad (2.12)$$

where  $m_{S(L)}$  and  $\Gamma_{S(L)}$  are the mass and decay width of the  $K_S^0$  ( $K_L^0$ ) mass eigenstates, and the parameters  $\chi$  and  $\bar{\chi}$  describe the material interaction of the  $K^0$  and  $\bar{K}^0$  flavour eigenstates. The  $\chi$  ( $\bar{\chi}$ ) parameter is proportional to the forward scattering amplitude of a  $K^0$  ( $\bar{K}^0$ ) meson in a traversed material. In Eq. (2.11),  $\psi_S^0$  and  $\psi_L^0$  are the initial  $K_S^0$  and  $K_L^0$  components of the neutral kaon state, which depend on the phase-space coordinates of the  $D$  decay:  $\psi_{S/L}^0 \propto \mathcal{A}_{S/L}(s_{-+})$ . Thus, for  $\Delta\chi \neq 0$ ,  $\psi_S(t)$  depends on  $\mathcal{A}_L(s_{+-})$  irrespective of the  $K_L^0 \rightarrow \pi^+\pi^-$  decay, due to kaon regeneration.

In addition, the relations  $A_S^{\bar{D}}(s_{-+}) = A_S^D(s_{+-})$  and  $A_L^{\bar{D}}(s_{-+}) = -A_L^D(s_{+-})$  are not exact for  $\epsilon \neq 0$ , as  $K_S^0$  and  $K_L^0$  are not exact  $CP$  eigenstates. This leads to further corrections to the yield expressions in Eq. (2.6). It is beneficial to express  $A_{S(L)}^D$  in terms of the amplitudes  $A_{1(2)}^D$ , defined analogously to Eq. (2.2) but for the  $CP$  even (odd) eigenstates  $K_1$  ( $K_2$ ). After the decay of a  $D^0$  meson to a neutral kaon, the kaon state is

$$\begin{aligned}\psi^0 &= A_1^D|K_1\rangle + A_2^D|K_2\rangle \\ &= N [(A_1^D - \epsilon A_2^D)|K_S^0\rangle + (A_2^D - \epsilon A_1^D)|K_L^0\rangle],\end{aligned}\quad (2.13)$$

with the normalisation constant  $N = \sqrt{1 + |\epsilon|^2}/(1 - \epsilon^2)$ . Thus it can be seen that

$$\begin{aligned}A_S^D(s_{+-}) &= N [(A_1^D(s_{+-}) - \epsilon A_2^D(s_{+-}))], \\ A_L^D(s_{+-}) &= N [(A_2^D(s_{+-}) - \epsilon A_1^D(s_{+-}))],\end{aligned}\quad (2.14)$$

with an analogous expression for the  $\bar{D}^0$  decay amplitudes. Therefore, the generalised relations between the  $D^0$  and  $\bar{D}^0$  amplitudes are

$$\begin{aligned}
A_S^{\bar{D}}(s_{+-}) &= N[A_1^{\bar{D}}(s_{+-}) - \epsilon A_2^{\bar{D}}(s_{+-})] \\
&= N[A_1^D(s_{-+}) + \epsilon A_2^D(s_{-+})] = A_S^D(s_{-+}) + 2N\epsilon A_2^D(s_{-+}), \\
A_L^{\bar{D}}(s_{+-}) &= N[A_2^{\bar{D}}(s_{+-}) - \epsilon A_1^{\bar{D}}(s_{+-})] \\
&= -N[A_2^D(s_{-+}) + \epsilon A_1^D(s_{-+})] = -A_L^D(s_{-+}) - 2N\epsilon A_1^D(s_{-+}).
\end{aligned} \tag{2.15}$$

In order to calculate the full corrections to the yield expressions in Eq. (2.6), models of  $A_S^D$  and  $A_L^D$  (or  $A_1^D$  and  $A_2^D$ ) are needed. While there are several amplitude models available to describe the decay amplitude  $A(D^0 \rightarrow K_S^0 \pi^+ \pi^-)$  [16–19, 39], no models have been published for  $D^0 \rightarrow K_L^0 \pi^+ \pi^-$  decays. However, following the assumptions laid out in Ref. [32], the amplitudes  $A_1^D(s_{+-})$  and  $A_2^D(s_{+-})$  can be related, allowing both qualitative and quantitative estimates of the bias effects to be made with existing  $D^0 \rightarrow K_S^0 \pi^+ \pi^-$  models. In the isobar formalism, the decay amplitude  $A(D^0 \rightarrow K_1 \pi^+ \pi^-)$  is expressed as a non-resonant constant amplitude plus a sum of resonances

$$A(D^0 \rightarrow K_1 \pi^+ \pi^-) = k_{NR} + \sum_{CF} k_i R^i(s_{K\pi^-}) + \sum_{DCS} k_j R^j(s_{K\pi^+}) + \sum_{R\pi\pi} k_k R^k(s_{\pi^+\pi^-}). \tag{2.16}$$

The resonances are split into Cabibbo-favoured (CF)  $K^{*-}$  resonances, doubly Cabibbo-suppressed (DCS)  $K^{*+}$  resonances and  $\pi\pi$  resonances. The  $R$  functions are taken to describe all kinematical dependence and are well described in eg. Refs. [17, 39] and references therein. In modern models, the  $\pi\pi$  and  $K\pi$   $S$ -wave components are modelled via the  $K$ -matrix formalism and LASS parametrisations, respectively, instead of sums of individual resonances [39]. This does not alter the arguments below, as the  $R$  functions of Eq. (2.16) can equally well represent such terms. The CF resonances couple to the  $\bar{K}^0$  component of  $K_1(\propto K^0 + \bar{K}^0)$ , and therefore the corresponding  $k_i$  in the  $K_2(\propto K^0 - \bar{K}^0)$  amplitude will have a relative minus sign. The DCS resonances couple to the  $K^0$  component of  $K_1$ , and so the corresponding  $k_j$  in the  $K_2$  amplitude will have a relative plus sign. For the  $h^+h^-$  resonances, there will be a coupling to both the  $K^0$  and  $\bar{K}^0$  components, however the coupling to the  $K^0$  component is expected to be suppressed with a Cabibbo suppression factor  $r_k e^{i\delta_k}$ , where  $r_k \simeq \tan^2 \theta_C \simeq 0.05$  is determined by the Cabibbo angle  $\theta_C$  and  $\delta_k$  can take any value. Therefore, the  $k_k$  for these resonances have a relative  $-(1 - 2r_k e^{i\delta_k})$  factor in the  $K_2$  amplitude. The same effect leads to the differences in decay rates between  $D^0 \rightarrow K_S^0 \pi^0$  and  $D^0 \rightarrow K_L^0 \pi^0$  decays [40, 41]. An important consequence of these substitution rules is that

$$A_2^D(s_{+-}) = -A_1^D(s_{+-}) + r_A \Delta A(s_{+-}), \tag{2.17}$$

where  $r_A \simeq \tan^2 \theta_C$  and  $\Delta A(s_{+-}) \sim A_1^D(s_{+-})$  are of the same order of magnitude (at least when averaged over the bins used in  $\gamma$  measurements). This relation is sufficient to make the qualitative arguments of Section 2.3, while the full set of substitution rules above are used in the quantitative studies of Section 3.

### 2.3 Impact on $\gamma$ measurements

With suitable models to calculate  $A_{S(L)}^{\overline{D}}$  (or  $A_{1/2}^{\overline{D}}$ ) and knowledge of  $\Delta\chi$  for the materials relevant to an experimental setting, Eqs. (2.10), (2.11), and (2.15) can be integrated to calculate the expected phase-space bin yields,  $N_i^\pm$ , including the effects of kaon  $CP$  violation and material interaction. Preliminary to doing this in Section 3, it is useful to look at the lowest order corrections to Eq. (2.6) in  $\epsilon$  and  $r_\chi = \frac{1}{2} \frac{\Delta\chi}{\Delta\lambda}$ , the dimensionless parameter governing material interactions. For LHCb and Belle II the average  $|r_\chi| \simeq 10^{-3}$ , as detailed in the Section 3. The studies of this section are made with the assumption of a flat phase-space efficiency and uniform acceptance over all decay times. Time-acceptance effects will be treated in Section 3. To first order in  $r_\chi$ , the expression in Eq. (2.11) simplifies to [38]

$$\begin{aligned}\psi_S(t, s_{+-}) &= e^{-\frac{i}{2}(\chi+\bar{\chi})t} e^{-i\lambda_S t} \left( \psi_S^0(s_{+-}) - r_\chi \left( 1 - e^{-i\Delta\lambda t} \right) \psi_L^0(s_{+-}) \right), \\ \psi_L(t, s_{+-}) &= e^{-\frac{i}{2}(\chi+\bar{\chi})t} e^{-i\lambda_L t} \left( \psi_L^0(s_{+-}) + r_\chi \left( 1 - e^{+i\Delta\lambda t} \right) \psi_S^0(s_{+-}) \right).\end{aligned}\quad (2.18)$$

In model-independent measurements, the  $K_i$  are obtained in a data-driven way using flavour-tagged  $D$  samples, and by averaging over  $D^0$  and  $\overline{D}^0$  decays. Therefore it proves beneficial to introduce the parameters

$$\hat{K}_i = \frac{1}{1 + |\epsilon + r_\chi|^2 \frac{\Gamma_S}{\Gamma_L}} \left( K_i^{(1)} + |\epsilon + r_\chi|^2 \frac{\Gamma_S}{\Gamma_L} K_i^{(2)} \right), \quad (2.19)$$

in which the  $K_i^{(1/2)}$  parameters are phase-space integrals, defined as in Eq. (2.7) but for  $A_{1/2}^D$ . The  $\hat{K}_i$  correspond to the expected measured value of  $K_i^{\text{meas}} = (N_i^D + N_{-i}^{\overline{D}}) / (\sum_j N_j^D + N_{-j}^{\overline{D}})$  to lowest order in  $\epsilon$  and  $r_\chi$ , where  $N_i^D$  ( $N_{-i}^{\overline{D}}$ ) is the expected yield of flavour tagged  $D^0$  ( $\overline{D}^0$ ) mesons into bin  $i$  of the  $D$  decay phase-space. In fits of amplitude models where both flavour tagged  $D^0$  and  $\overline{D}^0$  decays are used to fit the  $D \rightarrow K_S^0 \pi^+ \pi^-$  amplitude, related via Eq. (2.3), one will effectively fit an amplitude describing  $N_i^D + N_{-i}^{\overline{D}}$ , and therefore the arguments below, based on  $\hat{K}_i$ , will also hold for model-dependent measurements. Employing Eq. (2.17) in Eq. (2.19), the expected yields can be written

$$\begin{aligned}N_i^- &= h_B^{-'} \left( \hat{K}_{+i} + r_B^2 \hat{K}_{-i} + 2\sqrt{\hat{K}_{+i} \hat{K}_{-i}} (x_- \hat{c}_i + y_- \hat{s}_i) + O(r\epsilon) \right), \\ N_i^+ &= h_B^{+'} \left( \hat{K}_{-i} + r_B^2 \hat{K}_{+i} + 2\sqrt{\hat{K}_{+i} \hat{K}_{-i}} (x_+ \hat{c}_i - y_+ \hat{s}_i) + O(r\epsilon) \right),\end{aligned}\quad (2.20)$$

where  $O(r\epsilon)$  denotes terms of  $O(rA\epsilon)$ ,  $O(rB\epsilon)$ ,  $O(rAr_\chi)$ , and  $O(rBr_\chi)$ . Since  $r_B \sim r_A \sim 10^{-1}$  (in  $B^\pm \rightarrow DK^\pm$  decays) and  $r_\chi \sim \epsilon \sim 10^{-3}$ , these terms are all of the same order of magnitude. The new normalisation constants  $h_B^{\pm'} = h_B^\pm (1 + |\epsilon + r_\chi|^2 \frac{\Gamma_S}{\Gamma_L} \mp \Delta h)$  are defined in terms of

$$\Delta h = 2\text{Re}[\epsilon + r_\chi] - 4 \frac{\Gamma_S}{\Gamma_L + \Gamma_S} \frac{\text{Re}[\epsilon + r_\chi] + \mu \text{Im}[\epsilon + r_\chi]}{1 + \mu^2}, \quad \mu = 2 \frac{m_L - m_S}{\Gamma_L + \Gamma_S}. \quad (2.21)$$

The parameters  $(\hat{c}_i, \hat{s}_i)$  have been introduced to denote the *measured* average strong-phases, which are expected to differ from  $(c_i, s_i)$  at  $O(\epsilon)$ , since neutral kaon  $CP$  violation is not



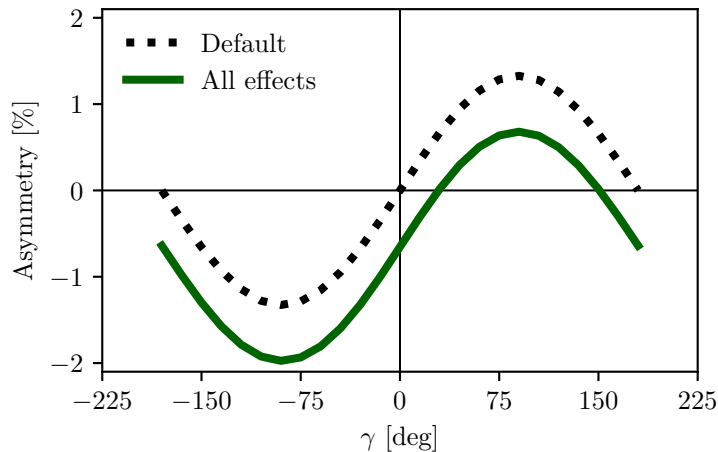


**Figure 2:** The asymmetry  $A_{\text{total}}$  as a function of  $\gamma$  calculated to  $O(\epsilon)$  using Eq. (2.22). The calculation is made using for (black dotted line) the default case where  $\Delta h = 0$  and (green) including neutral kaon  $CP$ -violation and material interaction with  $r_\chi = \epsilon$ .

taken into account in the measurements by CLEO. The corrections are thus in the neglected  $O(r_B\epsilon)$  terms.

Two observations can be made from the expression in (2.20). The first is that the phase-space *distribution* is only changed at  $O(r\epsilon)$  compared to the expression in Eq. (2.6), if the measured  $\hat{K}_i$  are used in the experimental analysis. As the  $D^0 - \bar{D}^0$  interference term that provides sensitivity to  $\gamma$  enters at order  $O(r_B)$ , the impact on  $\gamma$  measurements can be expected to be  $\Delta\gamma/\gamma \sim O(r\epsilon/r_B)$ . For  $B \rightarrow DK$  analyses, where  $r_B \simeq 0.1$ , this is at the permille level, so the induced  $\Delta\gamma$  bias can be expected to be smaller than  $1^\circ$ . This holds true, unless the integrated material interaction, and thereby effective  $r_\chi$ , varies significantly across the  $D$ -decay phase-space due to experimental effects. However, this is unlikely to be the case in practice, since no significant correlation between the phase-space coordinates and the travel direction of the kaon is expected.

The second observation relates to potential future measurements of  $\gamma$ , which may also include sensitivity from the total, phase-space-integrated yield asymmetry

$$A_{\text{total}} = \frac{N^- - N^+}{N^- + N^+} = \frac{2 \sum_i c_i \sqrt{\hat{K}_i \hat{K}_{-i}} r_B \sin \delta_B \sin \gamma + \Delta h}{1 + r_B^2 + 2 \sum_i c_i \sqrt{\hat{K}_i \hat{K}_{-i}} r_B \cos \delta_B \cos \gamma} + O(r\epsilon), \quad (2.22)$$

which was considered in Ref. [27]. In the limit  $r_B \rightarrow 0$  the expression agrees with the result for the analogous asymmetry in  $D^\pm \rightarrow \pi^\pm K_S^0$  decays in Ref. [42], evaluated to  $O(\epsilon)$  for an infinite and uniform time-acceptance. The asymmetry due to  $CP$  violation in the neutral kaon sector, governed by  $\Delta h$ , is of approximately the same order of magnitude as the asymmetry due to  $\gamma$  being non-zero. This is illustrated in Fig. 2, where the expression in Eq. (2.22) is plotted in the default case where  $\Delta h = 0$ , using the model in Ref. [39] to calculate  $K_i$  and  $c_i$ , as well as including neutral kaon  $CP$  violation and material interaction effects, calculated using  $r_\chi = \epsilon$ , with  $\epsilon$  taking the value in Eq. (2.9). The asymmetry changes

significantly when including the latter effects. Therefore, measurements based only on the global asymmetry will suffer relative biases of tens of degrees, not a few degrees, if neutral kaon  $CP$  violation and material interaction is not taken into account. The contribution to  $A_{\text{total}}$  due to  $CP$  violation in the  $B$  decay is an order of magnitude smaller than the  $O(r_B)$  expectation described in Ref. [27] because  $\sum_i c_i \sqrt{K_i K_{-i}} \simeq 0.1 \ll 1$ . The reason is that  $K_S^0 \pi^+ \pi^-$  is not a  $CP$  eigenstate and the strong-phase  $\Delta\delta_D(s_{-+})$  has a non-trivial phase-space dependence. This results in the CF and DCS interference term, which governs the  $CP$  asymmetry, changing sign over phase-space and therefore giving a small contribution to the phase-space-integrated yields.

### 3 Expected biases in LHCb and Belle II

In order to estimate the effects of  $CP$  violation and material interaction on  $\gamma$  measurements that are based on the phase-space distribution of signal decays, the equations of Section 2.2 need to be evaluated to at least  $O(r\epsilon)$ . Therefore a set of numerical studies are carried out, in which calculations are made to all orders in  $\epsilon$ ,  $r_\chi$ ,  $r_A$  and  $r_B$ . Furthermore, the bias effects depend on the specific detector material budget and time acceptance of a given experiment. The bias is calculated considering the conditions at the two main flavour physics experiments where measurements of  $\gamma$  will be performed in the next decade: LHCb and Belle II.

#### 3.1 Time acceptance, momentum distribution, and material parameters

Experiment specific biases are obtained for LHCb and Belle II, by assuming time acceptances, momentum distributions, and detector geometries typical of the experiments. The LHCb experiment is a forward arm spectrometer where the  $B$  mesons are produced in proton-proton collisions at 13 TeV. Subsequent decays of the  $K_S^0$  are highly boosted and can occur within different detector subsystems, which leads to two distinct categories of candidates, with different mean lifetimes and material traversed. Therefore two scenarios are considered for LHCb: one in which the decay products of the  $K_S^0$  leave reconstructed tracks in both the silicon vertex detector and downstream tracking detectors (denoted *long-long* or LL), and one in which the decay products of the  $K_S^0$  only leave tracks in the downstream tracking detectors (denoted *down-down* or DD). At Belle II,  $B$  mesons are produced from decays of  $\Upsilon(4S)$  mesons, produced in asymmetric electron-positron collisions. This leads to substantially different decay kinematics in comparison to those found at LHCb. A single scenario is considered for Belle II, because nearly all the  $K_S^0$  mesons produced in signal decays in Belle II decay within the tracking volume, with more than 90% decaying in the vertex detector according to the studies described below. Thus, three scenarios are considered in total: LL LHCb, DD LHCb, and Belle II.

In order to model the experimental time acceptance, the time-dependent integral in Eq. (2.10) is only carried out over a finite time interval  $(\tau_1, \tau_2)$ . The intervals are defined for each of the three experimental categories, by requiring that a neutral kaon, if produced at  $x = y = z = 0$  with momentum  $p = (p_T, p_z)$ , decays within the relevant part of the corresponding detector. The time acceptance has a significant impact for the LHCb categories,

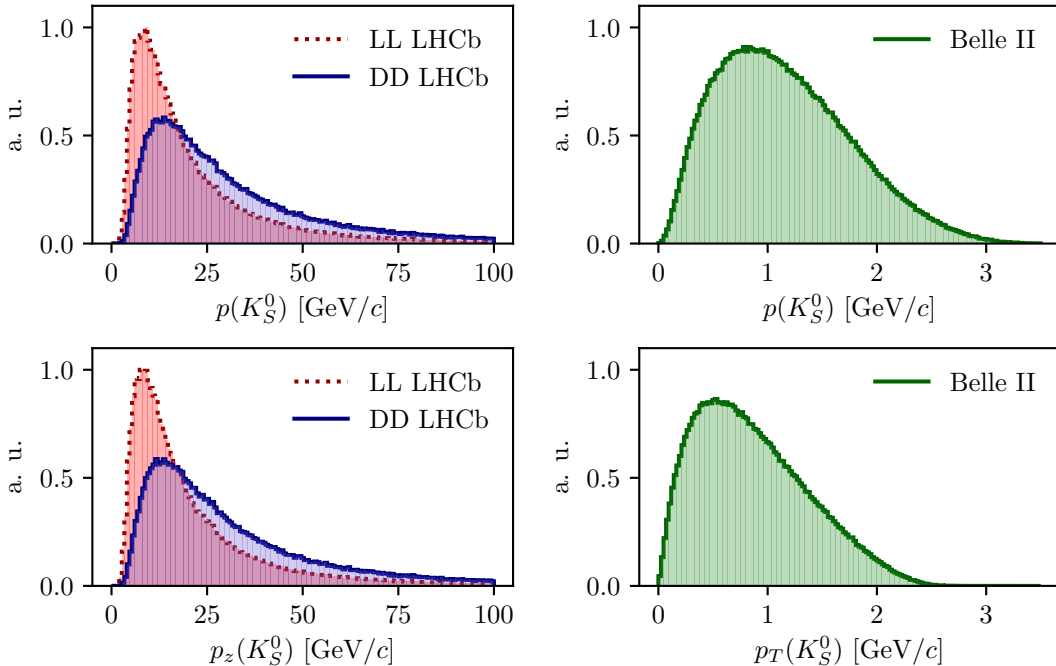


**Figure 3:** Momentum distributions for the LHCb (red dotted line) LL and (blue) DD categories, as well as (green) Belle II, obtained using `RapidSim`.

where some 20% of the kaons escape the tracking stations completely before decaying, whereas the resulting cut-off,  $\tau_2$ , is large enough in Belle II to have negligible significance. A discussion on the exact requirements placed, and corresponding decay lengths, is found in appendix A.

The neutral kaon momentum distribution in LHCb is obtained using `RapidSim` [43], which can generate decays of  $B$  mesons with the kinematic distribution found in LHCb collisions, and falling in the LHCb acceptance. The momentum distribution in Belle II is estimated by decaying  $B$  mesons with a momentum of 1.50 GeV/ $c$  along the  $z$ -axis using `RapidSim`, corresponding to the  $\gamma\beta = 0.28$  boost of the centre-of-mass system in Belle II when operated at the  $\Upsilon(4S)$  resonance [26]. A perfect  $4\pi$  angular acceptance is assumed. The generated  $D \rightarrow K_S^0 \pi^+ \pi^-$  decays are uniformly distributed in phase space. The `RapidSim` samples for LHCb are reweighted to take the relevant time acceptance into account. This is not necessary for Belle II, as all produced  $K_S^0$  mesons decay in the tracking volume. The resulting momentum distributions for the three types of sample are shown in Fig. 3.

The parameter  $\Delta\chi$  describes the matter-interaction effect, as detailed in Section 2.2. It depends on kaon momentum and varies along a given kaon path, as the kaon intersects detector components made of different materials. In these studies, the calculations are simplified by using a constant set of average material parameters for each experimental scenario.

The average material parameters can be estimated for a given experimental scenario by considering the type and length of material traversed by a kaon in the relevant sub-detector(s). A detailed description of the calculation is given in appendix A. The average value of the dimensionless parameter  $r_\chi = \frac{1}{2} \frac{\Delta\chi}{\Delta\lambda}$ , which governs the size of the matter regeneration effect, can be calculated for the three considered experimental scenarios, and the averages are found to satisfy  $|r_\chi^{\text{LL}}| = 2.7 \times 10^{-3}$ ,  $|r_\chi^{\text{DD}}| = 2.2 \times 10^{-3}$ , and  $|r_\chi^{\text{Belle II}}| = 1.0 \times 10^{-3}$ .

The LHCb detector is undergoing a significant upgrade prior to the start of the LHC Run 3. However, the material budget and geometry of the relevant sub-detectors will be similar to the sub-detectors used during Run 1 and 2 [44, 45]. Hence the results of this study will be valid for measurements during the upgrade phases of LHCb, even though the detector parameters presented in this section relate to the original LHCb detector.

### 3.2 Calculation procedure

In the numerical bias studies, the amplitude model for  $D^0 \rightarrow K_S^0 \pi^+ \pi^-$  decays in Ref. [39] is taken to represent the  $A_1(s_{+-})$  amplitude. Then  $A_2(s_{+-})$  is obtained as described in Section 2.2. In terms of  $A_1$  and  $A_2$ , the amplitudes  $A_{S(L)}^{\bar{D}}(s_{+-})$  can be expressed and related via Eqs. (2.14) and (2.15), and the full  $\mathcal{A}_{S/L}^\pm(s_{+-})$  amplitudes calculated for a given set of input parameters  $(\gamma^0, r_B^0, \delta_B^0)$ . Then Eq. (2.11) gives the kaon state as a function of time, phase-space coordinates, and the material parameter  $\Delta\chi$ . The neutral kaon state components,  $\psi_S(t)$  and  $\psi_{\bar{S}}(t)$ , are inserted into Eq. (2.10), which is integrated numerically over time and the phase-space bins of Fig. 1 to obtain the expected yields in each bin. These integrals use the experimental time acceptance that was described in Section 3.1. The signal yields depend on the momentum via the time-acceptance parameters  $\tau_1$  and  $\tau_2$ , and because the material interaction parameter  $\Delta\chi$  is momentum dependent. Therefore, the yields are averaged over the  $K_S^0$  momentum distributions of LHCb and Belle II. The neutral kaon momentum in the lab frame is correlated with  $m^2(\pi^+ \pi^-)$ , and in order to take this correlation into account in the averaging, the kaon  $p$ ,  $p_z$ , and  $p_T$  distributions are extracted for a number of different  $m^2(\pi^+ \pi^-)$  values, using the `RapidSim` samples described in Section 3.1. In order to keep the calculations manageable, the distributions of kaon  $p$ ,  $p_z$ , and  $p_T$  for each phase-space point are divided into 5 quantiles and the 5 medians of these quantiles are used to represent the overall distribution.

The parameters  $x_\pm$  and  $y_\pm$  are determined by a maximum likelihood fit to the calculated yields, using the default yield expression in Eq. (2.6), which ignores the presence of  $CP$  violation and material interaction in the neutral kaon sector. The fit result and covariance matrix are interpreted in terms of the physics parameters  $(\gamma, r_B, \delta_B)$  using another maximum likelihood fit [4], to allow for the extraction of the bias  $\Delta\gamma = \gamma - \gamma^0$ . In the fits, the  $K_i$  are obtained using the definition  $K_i = K_i^{\text{meas}} = (N_i^D + N_{-i}^{\bar{D}}) / (\sum_j N_j^D + N_{-j}^{\bar{D}})$ , in terms of the expected yields  $N_i^D$  ( $N_i^{\bar{D}}$ ) of a flavour-tagged  $D^0$  ( $\bar{D}^0$ ) decays in bin  $i$  of the  $D$  decay phase space, calculated as described above for  $r_B^0 = 0$ . This corresponds to experimentally measuring the  $K_i$  in a control channel, and takes the effect of neutral kaon  $CP$  violation and material interaction on  $K_i$  measurements into account, as well the experimental time acceptance. The  $(c_i, s_i)$  are calculated using  $A_1(s_{+-})$  and the experimental time

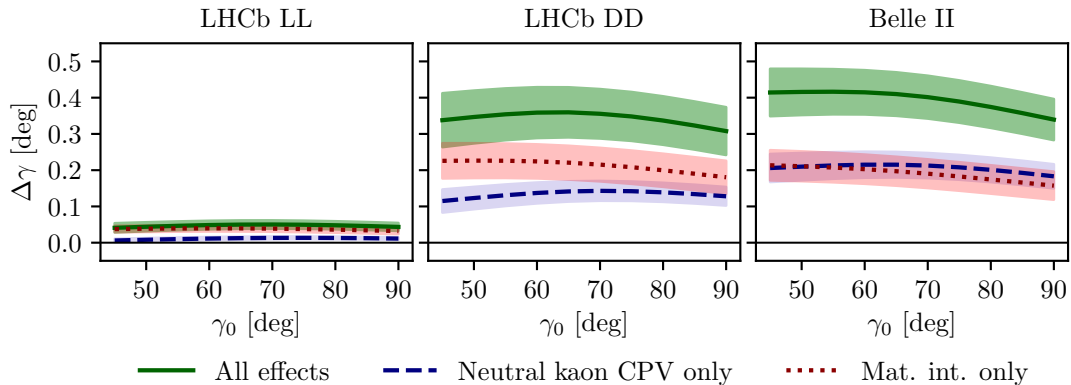


**Figure 4:** The bias  $\Delta\gamma$  as a function of input  $\gamma_0$  for (left) the LL LHCb category, (centre) the DD LHCb category, and (right) Belle II. The bias is calculated due to (blue, dashed line) neutral kaon  $CP$  violation alone, (red, dotted line) material interaction alone, and (green line) both effects. The shaded region shows the estimated  $1\sigma$  uncertainty band.

acceptance is taken into account in this calculation as well. While a model-independent method is specifically used here to determine biases, it is expected that traditional and new unbinned methods such as those in Refs [14–20] and Ref. [46], respectively, will be similarly biased if the kaon  $CP$ -violation and regeneration are not accounted for.

### 3.3 Results

The obtained bias  $\Delta\gamma$  is shown as a function of input  $\gamma^0$  for the various experimental conditions in Fig. 4. The calculations are made using  $(r_B^0, \delta_B^0) = (0.1, 130^\circ)$ , approximately equal to the physics parameters relevant for  $B^\pm \rightarrow DK^\pm$  decays [6, 7]. The bias does not vary significantly with  $\gamma^0$  in the plotted range, which includes the world average value of direct  $\gamma$  measurements as well as the values obtained in full unitarity-triangle fits [6–8], and for all cases, the bias is found to be below  $0.5^\circ$ , corresponding to relative biases of about half a percent. Thus the biases are of  $O(r\epsilon/r_B)$  as expected, given the arguments of Section 2. The contributions from the individual  $K_S^0$   $CPV$  and material interaction effects are also shown. It is seen that the neutral kaon  $CP$  violation and material interaction effects leads to approximately equal biases in all three cases.

Given the decay-time acceptance and momentum distribution for each experimental category, the mean life time,  $\langle\tau\rangle$ , of the reconstructed kaons can be calculated. In terms of the  $K_S^0$  lifetime  $\tau_{K_S^0} = (0.895 \pm 0.004) \times 10^{-11}$  s [35],  $\langle\tau_{LL}\rangle \simeq 0.1\tau_{K_S^0}$  for the LHCb LL category,  $\langle\tau_{DD}\rangle \simeq 0.8\tau_{K_S^0}$  for the LHCb DD category, and at Belle II  $\langle\tau_{Belle\ II}\rangle \simeq \tau_{K_S^0}$ . The difference in average kaon lifetime is reflected in the observed biases, which are found to be larger in the samples with longer lived kaons. The very small effect in the LL category is to be expected because the  $CP$ -violation effect due to  $K_S^0$  not being  $CP$ -even is approximately cancelled by the  $CP$ -violation effect arising from  $K_S^0 - K_L^0$  interference for kaons with decay times much smaller than  $\tau_{K_S^0}$  [42]. The time dependence of the bias effect means that it can potentially be beneficial to restrict a measurement to using short-lived  $K_S^0$  mesons in

a future scenario, where the impact of  $K_S^0$   $CP$  violation is comparable to the statistical precision of the measurement. For example, the bias can be reduced by 40% in the Belle II scenario if only  $K_S^0$  mesons decaying within 8 cm of the beam axis are included in the measurement. This requirement only removes 20% of the signal yield, and hence only increases the statistical uncertainty of the measurement by 10%.

The uncertainty bands in Fig. 4 are calculated by repeating the study while varying some of the inputs. The model dependence of the predicted biases is probed by repeating the study using two other amplitude models as input for  $A_1(s_{+-})$  and  $A_2(s_{+-})$ : the model published in Ref. [16] and the model included in EVTGEN [47]. The use of different models change the predicted biases by up to  $0.05^\circ$ . When defining  $A_2(s_{+-})$  in terms of  $A_1(s_{+-})$ , there is an uncertainty due to the unknown  $(r_k, \delta_k)$  parameters used to describe the  $\pi\pi$  resonance terms. This uncertainty is assessed by making the study with 50 different random realisations of the parameter set. The phases  $\delta_k$  are sampled uniformly in the interval  $[0, 2\pi]$  while the  $r_k$  are sampled from a normal distribution with  $\mu = \tan^2 \theta_C$  and  $\sigma = \mu/2$ . The uncertainty is about  $0.05^\circ$  across the three experiments considered. The studies are repeated while varying the time acceptances and material densities with  $\pm 10\%$ . The largest deviations in biases are found to be below  $0.05^\circ$ . The dependence on the handling of the momentum distribution is estimated by repeating the study using 10 and 20 quantiles to describe the momentum distributions at each point in phase space, instead of 5. The variation in the results is taken as the systematic uncertainty, and found to be below  $0.01^\circ$  for all experiments. There is an additional uncertainty due to the use of simulation samples generated with RapidSim to describe the kaon momentum distribution, in lieu of full detector simulations. The uncertainty has not been considered here. Full detector simulation should be used if specific experimental measurements are to be corrected for the biases described in this study.

There is also an uncertainty from the use of  $(c_i, s_i)$  as calculated using  $A_1(s_{+-})$ . It is to be expected that the measured values  $(\hat{c}_i, \hat{s}_i)$  from the CLEO collaboration differ by those calculated using  $A_1^D(s_-, s_+)$  by terms of  $O(\epsilon)$  due to neutral kaon  $CP$  violation, which is not taken into account in the measurement [32]. These corrections can be calculated via a procedure analogous to the one used to estimate the corrections on measurements of  $\gamma$  in this paper. However, as these corrections are much smaller than the experimental uncertainties in the measurement, they have not been studied further.

It is interesting to evaluate the bias obtained if the  $K_i$  are calculated from  $A_1(s_{+-})$ , without any corrections due to neutral kaon  $CP$  violation and material interaction. If this is done, while the full experimental time acceptance is taken into account, the biases only change by up to  $0.01^\circ$ , across the experiments. This is because the  $O(\epsilon)$  corrections in Eq. (2.19), where the expected measured  $K_i$  is given to lowest order in  $\epsilon$  and  $r_\chi$ , only affect the overall normalisation. If the time acceptance is *not* taken into account, biases of several degrees can occur, irrespective of the presence of neutral kaon  $CP$  violation or material interaction effects.

While the  $B^\pm \rightarrow DK^\pm$  decay mode provides the best sensitivity to  $\gamma$ , it is also possible to measure  $\gamma$  in other  $B$  decay channels, such as  $B^\pm \rightarrow D^*K^\pm$ ,  $B^\pm \rightarrow DK^{*\pm}$ ,  $B^0 \rightarrow DK^{*0}$ , and  $B^\pm \rightarrow D\pi^\pm$ . For the purpose of the study presented here, the main difference between

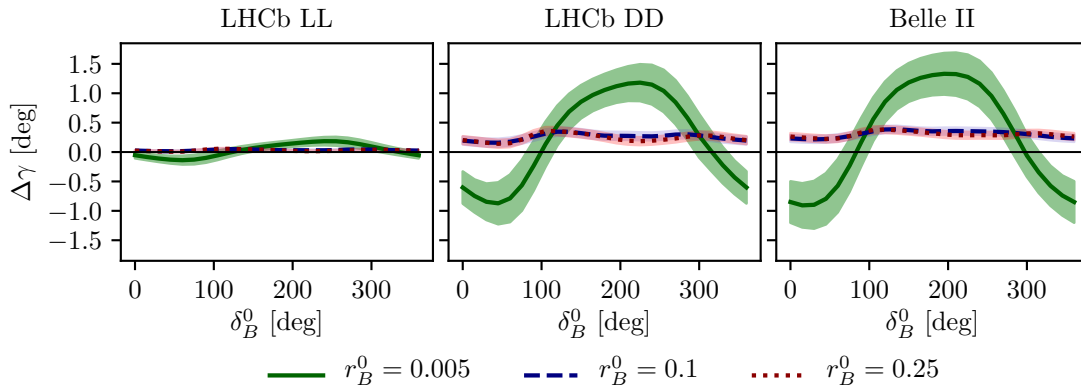


**Figure 5:** The bias  $\Delta\gamma$  as a function of input  $\delta_B$  for (left) the LL LHCb category, (centre) the DD LHCb category, and (right) Belle II. The bias is calculated for  $\gamma = 75^\circ$  and (green line)  $r_B = 0.005$ , (blue, dashed line)  $r_B = 0.1$ , and (red, dotted line)  $r_B = 0.25$ . The shaded region shows the estimated  $1\sigma$  uncertainty band.

the decay channels is that they have different values of  $r_B$  and  $\delta_B$ . Figure 5 shows  $\Delta\gamma$  as a function of input  $\delta_B^0$ , for  $\gamma^0 = 75^\circ$  and three different values of  $r_B^0$ . Aside from  $r_B^0 = 0.1$ , the results are shown for  $r_B^0 = 0.005$ , which corresponds to the expectation in  $B^\pm \rightarrow D\pi^\pm$  decays [48] and  $r_B^0 = 0.25$ , which corresponds to  $B^0 \rightarrow DK^{*0}$  decays [4, 5]. Three features are notable, namely that the biases depend on  $\delta_B^0$ , that the biases are large for the small  $r_B^0 = 0.005$  case, and that the oscillation period of the  $\delta_B$  dependence is different between the  $r_B^0 = 0.005$  case and the  $r_B^0 \in \{0.1, 0.25\}$  cases. It is to be expected that  $\Delta\gamma$  oscillates as a function of  $\delta_B^0$ , because  $\delta_B^0$  enters the yield equations via  $\cos(\delta_B^0 \pm \gamma)$  and  $\sin(\delta_B^0 \pm \gamma)$  terms. The  $r_B^0$  dependent behaviour is governed by the relative importance of different  $O(r\epsilon)$  correction terms to the phase-space distribution. There are terms of both  $O(r_A\epsilon)$  and  $O(r_B\epsilon)^2$ , which lead to expected biases of size  $O(r_A\epsilon/r_B)$  and  $O(r_B\epsilon/r_B) = O(\epsilon)$ , respectively, cf. the discussion of Section 2.3. The  $O(r_A\epsilon)$  terms are independent of  $\delta_B^0$ , whereas the  $O(r_B\epsilon)$  terms have factors of  $\cos(\delta_B^0 \pm \gamma)$  and  $\sin(\delta_B^0 \pm \gamma)$ . Therefore the  $O(r_A\epsilon)$  and  $O(r_B\epsilon)$  terms introduce biases with different dependence on  $\delta_B^0$ . In the  $B^\pm \rightarrow D\pi^\pm$  case, the  $O(r_A\epsilon)$  correction terms dominate because  $r_A/r_B \simeq (0.05/0.005) = 10$ . This explains the relatively large bias, as  $|r_A\epsilon/r_B^{D\pi}| \simeq 4\%$ , and the simple dependence on  $\delta_B^0$ . The bias is seen to be up to  $\pm 1.5^\circ$ , but only about  $+0.2^\circ$  with the expected value of  $\delta_B^{D\pi} \simeq 300^\circ$  [4, 48]. In the  $r_B^0 = 0.1$  and  $r_B^0 = 0.25$  cases the  $O(r_B\epsilon)$  correction terms dominate, and the biases are of  $O(\epsilon)$ , independent of the  $r_B^0$  value. Therefore both cases have biases of similar size and with similar  $\delta_B^0$  dependence. While the input value of  $\gamma^0 = 75^\circ$  was chosen for these studies, there is minimal variation in the results if another value of  $\gamma^0$  in the range  $[65^\circ, 85^\circ]$  is used.

The  $\gamma$  measurements treated in this paper can be made using other  $D$ -decay final states,

<sup>2</sup>There are similar terms of  $O(r_A r_\chi)$  and  $O(r_B r_\chi)$ , but as  $\epsilon$  and  $r_\chi$  are of the same order of magnitude, these terms can be treated completely analogously to the  $O(r_A\epsilon)$  and  $O(r_B\epsilon)$  terms, and have been left out of the discussion for brevity.

such as  $D \rightarrow K_S^0 K^+ K^-$  and  $D \rightarrow K_S^0 \pi^+ \pi^- \pi^0$ . The biases from neutral kaon  $CP$  violation and material interaction on measurements of  $\gamma$  based the  $D$  decay phase-space distributions should be of similar size in these decay channels, as those presented for  $D \rightarrow K_S^0 \pi^+ \pi^-$  in this paper. The impact on  $\gamma$  measurements based on the phase-space-integrated yield asymmetry can be expected to be tens of degrees for the  $D \rightarrow K_S^0 K^+ K^-$  channel, where the yield asymmetry is expected to be around 2%, for the reasons explained in Section 2.3. The  $D \rightarrow K_S^0 \pi^+ \pi^- \pi^0$  decay, however, is dominantly  $CP$ -odd [49], and the bias in measurements based on the total asymmetry is therefore expected to be  $O(r_B \epsilon)$ , ie. a few degrees [27]. More precise calculations of the biases would require a repeat of the study included here, with relevant amplitude models and binning schemes in place.

The studies presented here can be used to assign systematic uncertainties to measurements while the statistical uncertainties continue to dominate. As the statistical uncertainty becomes comparable with the bias effects described in this paper, the systematic uncertainty should be assigned by repeating the studies with a detailed detector simulation. This would incorporate a more accurate description of the  $K_S^0$  decay-time acceptance, of the full selection criteria, and the traversed material. The detailed calculations can also be used to apply a bias correction if desired.

## 4 Conclusion

$CP$  violation and material interaction of neutral kaons constitute sources of bias in measurements of the CKM angle  $\gamma$  based on  $B^\pm \rightarrow D(\rightarrow K_S^0 \pi^+ \pi^-) K^\pm$  decays. The relative induced bias due to these effects has been shown to be of permille level for measurements based on the difference in distributions over the  $D$  decay phase space between signal decays originating from  $B^+$  and  $B^-$  mesons. However, measurements based only on the phase-space-integrated yield asymmetry between  $B^+$  and  $B^-$  decays, have been show to suffer biases as large as tens of degrees. The expected biases in measurements based on the phase-space distribution have been estimated for experimental conditions corresponding to LHCb and Belle II and found to be below  $0.5^\circ$ , which is smaller than the precision the experiments expect to reach in this decay mode during their lifetimes.

## Acknowledgments

We thank Markus Röhrken for providing an implementation of the latest amplitude model, Jim Libby for his helpful consultation on the Belle II detector, and Guy Wilkinson for stimulating discussions. We are grateful for support from the Royal Society, the ERC, the Louis-Hansen Foundation, Knud Højgaard’s Foundation and the Augustinus Foundation.

## A Details of the detector parameterisation

To model the decay-time acceptance, requirements are placed on where the neutral kaon can decay within the detector. At LHCb the relevant detector components are the silicon vertex detector closest to the beam pipe (the VELO) and the ring-imaging Cherenkov detector



which is positioned in between the VELO and the downstream trackers (the RICH1). For the LL LHCb category, it is required that the kaon decays before reaching  $z_{max} = 280$  mm, corresponding to a decay where the decay products traverse at least 3 VELO segments (ignoring a number of widely spaced VELO segments placed at a distance of up to  $z = 750$  mm from the interaction point) [50]. For the DD LHCb category a decay at  $z \in [280, 2350]$  mm is required, corresponding to decay between the LL cut-off and the first downstream tracking station [51]. For Belle II, it is assumed that the  $K_s^0$  reconstruction is similar to the Belle  $K_s^0$  reconstruction, which is based on a neural network and reconstructs  $K_s^0$  decays for which the decay product leave tracks in the drift chamber only, as well as decays with decay products that leave tracks in both the drift chamber and silicon vertex detectors [52, 53]. Therefore, the  $K_s^0$  decay is required to be within  $r_{max} = 1130$  mm of the beam axis, corresponding to a decay within the outer radius of the drift-chamber [26]. In practice, most of the kaons decay inside the silicon vertex detector, the outermost layer of which is at  $r = 140$  mm [26], so requiring a decay before 1130 mm is essentially equivalent to having no time cut-off.

The parameter  $\Delta\chi$  that describes the material interaction in Eq. (2.11) is related to the forward scattering amplitude  $f$  ( $\bar{f}$ ) of  $K^0$  ( $\bar{K}^0$ ) mesons in a given material [37, 38]

$$\Delta\chi = -\frac{2\pi\mathcal{N}}{m_K}(f - \bar{f}) = -\frac{2\pi(N_A\rho/A)}{m_K}(f - \bar{f}), \quad (\text{A.1})$$

where  $\mathcal{N} = N_A\rho/A$  is the scattering centre density of the material,  $m_K$  is the mass of the kaon state,  $A$  and  $\rho$  are the nucleon number and density of the material, and  $N_A$  is Avogadro's number. Measurements made for a range of nuclei [54] show that in the momentum range  $p_K \in [20, 140]$  GeV/ $c$

$$\left| \frac{f - \bar{f}}{p_K} \right| = 2.23 \frac{A^{0.758}}{p_K^{0.614} (\text{GeV}/c)} \text{ mb}, \quad \arg[f - \bar{f}] = -\frac{\pi}{2} (2 - 0.614), \quad (\text{A.2})$$

where the phase of  $\Delta f$  is determined via a phase-power relation [55]. In the numerical studies presented here, Eq. (A.2) is also used for the low momentum neutral kaons in the Belle II calculations, as a more detailed modelling of the low momentum  $\Delta\chi$  based on Ref. [56] is found to yield very similar results. The scattering centre density  $\mathcal{N}$  is approximated as being constant, equal to the average density along a neutral kaon path due to its intersection with different detector segments. This average is estimated using the simplifying assumption that the total detector material budget is due to silicon. In practice,  $\mathcal{N} = N_A\rho/A$  is calculated using  $A = 28$  and  $\rho = f^{\text{Si}}\rho^{\text{Si}}$ , where  $f^{\text{Si}} < 1$  is the average fraction of a neutral kaon path length that is inside detector material, estimated via the known dimensions of the detector, the average nuclear interaction length seen by a track traversing it, and the nuclear interaction length of silicon  $\lambda_I^{\text{Si}} = 465.2$  mm [35]. To calculate the average material density for the LL LHCb category, the full length of the VELO,  $L_{\text{VELO}} = 750$  mm, is used, as the average  $\Delta x/\lambda_I = 3.8\%$  is given for particles traversing the whole detector in Ref. [50]. The calculation yields  $f_{\text{L}}^{\text{Si}} = (\Delta x/\lambda_I) \times \lambda_I^{\text{Si}}/L_{\text{VELO}} = 2.4\%$ .

The corresponding number in the DD category, in which the neutral kaons traverse both the VELO and the RICH1 detector, is obtained by assuming that the space be-

tween  $z = 750$  mm and  $z = 2350$  mm is taken by the RICH1, in which the average nuclear interaction length seen is  $\Delta x/\lambda_I = 2.6\%$  [57]. Averaging the density between the VELO and RICH1 detectors yields  $f_{\text{DD}}^{\text{Si}} = 1.6\%$  (the average is weighted with a factor,  $\exp[-t/\tau_{K_S^0}] = \exp[-zm_K/(\tau_{K_S^0} p_{K_S^0})]$ , using the mean  $K_S^0$  momentum, to take into account that more  $K_S^0$  mesons decay earlier, where the density is higher, rather than later).

In Belle II the particle travels approximately 6 % of a radiation length in the beam pipe and vertex detectors [58], which stretch to  $r = 140$  mm [26], and another 6 % of a radiation length in the drift chamber [58] (using the approximate material budget in the central region  $\theta \in [35^\circ, 120^\circ]$ ), which stretches to  $r = 1130$  mm [26]. A calculation analogous to those above, but using the radiation length of silicon  $X_0^{\text{Si}} = 93.7$  mm [35], yields  $f_{\text{Belle II}}^{\text{Si}} = 3.8\%$ . As for the LHCb calculations, the full radial length of the detector segments are used because the material budget is given for tracks traversing the whole detector, and the average is calculated with a weight factor of  $\exp[-zm_K/(\tau_{K_S^0} p_{K_S^0})]$ .

The average value of  $r_\chi = \frac{1}{2} \frac{\Delta\chi}{\Delta\lambda}$ , which governs the size of the matter regeneration effect, can be calculated for the three considered experimental scenarios and satisfy  $|r_\chi^{\text{LL}}| = 2.7 \times 10^{-3}$ ,  $|r_\chi^{\text{DD}}| = 2.2 \times 10^{-3}$ , and  $|r_\chi^{\text{Belle II}}| = 1.0 \times 10^{-3}$ .

## References

- [1] N. Cabibbo, *Unitary symmetry and leptonic decays*, *Phys. Rev. Lett.* **10** (1963) 531.
- [2] M. Kobayashi and T. Maskawa, *CP-violation in the renormalizable theory of weak interaction*, *Prog. Theor. Phys.* **49** (1973) 652.
- [3] M. Blanke and A. J. Buras, *Emerging  $\Delta M_d$  -anomaly from tree-level determinations of  $|V_{cb}|$  and the angle  $\gamma$* , *Eur. Phys. J.* **C79** (2019) 159 [1812.06963].
- [4] LHCb COLLABORATION, R. Aaij et al., *Measurement of the CKM angle  $\gamma$  from a combination of LHCb results*, *JHEP* **12** (2016) 087 [1611.03076].
- [5] LHCb COLLABORATION, M. W. Kenzie and M. P. Whitehead, *Update of the LHCb combination of the CKM angle  $\gamma$* , LHCb-CONF-2018-002, 2018.
- [6] HEAVY FLAVOR AVERAGING GROUP, Y. Amhis et al., *Averages of  $b$ -hadron,  $c$ -hadron, and  $\tau$ -lepton properties as of summer 2016*, *Eur. Phys. J.* **C77** (2017) 895 [1612.07233].
- [7] UTFIT COLLABORATION, M. Bona et al., *The unitarity triangle fit in the standard model and hadronic parameters from lattice QCD: A reappraisal after the measurements of  $\Delta m_s$  and  $BR(B \rightarrow \tau\nu_\tau)$* , *JHEP* **10** (2006) 081 [hep-ph/0606167].
- [8] CKMFITTER GROUP, J. Charles et al., *Current status of the Standard Model CKM fit and constraints on  $\Delta F = 2$  new physics*, *Phys. Rev.* **D91** (2015) 073007 [1501.05013].
- [9] A. Bondar, *Proceedings of BINP special analysis meeting on Dalitz analysis, 24-26 Sep. 2002, unpublished*.
- [10] A. Bondar and A. Poluektov, *Feasibility study of model-independent approach to  $\phi_3$  measurement using Dalitz plot analysis*, *Eur.Phys.J.* **C47** (2006) 347 [hep-ph/0510246].
- [11] A. Bondar and A. Poluektov, *The use of quantum-correlated  $D^0$  decays for  $\phi_3$  measurement*, *Eur.Phys.J.* **C55** (2008) 51 [0801.0840].

- [12] A. Giri, Y. Grossman, A. Soffer and J. Zupan, *Determining  $\gamma$  using  $B^\pm \rightarrow DK^\pm$  with multibody  $D$  decays*, *Phys. Rev.* **D68** (2003) 054018 [[hep-ph/0303187](#)].
- [13] BELLE COLLABORATION, H. Aihara et al., *First measurement of  $\phi_3$  with a model-independent Dalitz plot analysis of  $B^\pm \rightarrow DK^\pm$ ,  $D \rightarrow K_S^0 \pi^+ \pi^-$  decay*, *Phys. Rev.* **D85** (2012) 112014 [[1204.6561](#)].
- [14] BELLE COLLABORATION, A. Poluektov et al., *Measurement of  $\phi_3$  with Dalitz plot analysis of  $B^\pm \rightarrow D^{(*)}K^\pm$  decay*, *Phys.Rev.* **D70** (2004) 072003 [[hep-ex/0406067](#)].
- [15] BELLE COLLABORATION, A. Poluektov et al., *Measurement of  $\phi_3$  with Dalitz plot analysis of  $B^+ \rightarrow D^{(*)}K^{(*)+}$  decay*, *Phys.Rev.* **D73** (2006) 112009 [[hep-ex/0604054](#)].
- [16] BELLE COLLABORATION, A. Poluektov et al., *Evidence for direct CP violation in the decay  $B^\pm \rightarrow D^{(*)}K^\pm$ ,  $D \rightarrow K_S^0 \pi^+ \pi^-$  and measurement of the CKM phase  $\phi_3$* , *Phys.Rev.* **D81** (2010) 112002 [[1003.3360](#)].
- [17] BABAR COLLABORATION, B. Aubert et al., *Measurement of the Cabibbo-Kobayashi-Maskawa angle  $\gamma$  in  $B^\mp \rightarrow D^{(*)}K^\mp$  decays with a Dalitz analysis of  $D \rightarrow K_S^0 \pi^- \pi^+$* , *Phys.Rev.Lett.* **95** (2005) 121802 [[hep-ex/0504039](#)].
- [18] BABAR COLLABORATION, B. Aubert et al., *Improved measurement of the CKM angle  $\gamma$  in  $B^\mp \rightarrow D^{(*)}K^{(*)\mp}$  decays with a Dalitz plot analysis of  $D$  decays to  $K_S^0 \pi^+ \pi^-$  and  $K_S^0 K^+ K^-$* , *Phys.Rev.* **D78** (2008) 034023 [[0804.2089](#)].
- [19] BABAR COLLABORATION, P. del Amo Sanchez et al., *Evidence for direct CP violation in the measurement of the Cabibbo-Kobayashi-Maskawa angle  $\gamma$  with  $B^\mp \rightarrow D^{(*)}K^{(*)\mp}$  decays*, *Phys.Rev.Lett.* **105** (2010) 121801 [[1005.1096](#)].
- [20] LHCb COLLABORATION, R. Aaij et al., *Measurement of CP violation and constraints on the CKM angle  $\gamma$  in  $B^\pm \rightarrow DK^\pm$  with  $D \rightarrow K_S^0 \pi^+ \pi^-$  decays*, *Nucl. Phys.* **B888** (2014) 169 [[1407.6211](#)].
- [21] LHCb COLLABORATION, R. Aaij et al., *Measurement of the CKM angle  $\gamma$  using  $B^0 \rightarrow DK^{*0}$  with  $D \rightarrow K_S^0 \pi^+ \pi^-$  decays*, *JHEP* **08** (2016) 137 [[1605.01082](#)].
- [22] LHCb COLLABORATION, R. Aaij et al., *Measurement of the CKM angle  $\gamma$  using  $B^\pm \rightarrow DK^\pm$  with  $D \rightarrow K_S^0 \pi^+ \pi^-$ ,  $K_S^0 K^+ K^-$  decays*, *JHEP* **10** (2014) 097 [[1408.2748](#)].
- [23] LHCb COLLABORATION, R. Aaij et al., *Model-independent measurement of the CKM angle  $\gamma$  using  $B^0 \rightarrow DK^{*0}$  decays with  $D \rightarrow K_S^0 \pi^+ \pi^-$  and  $K_S^0 K^+ K^-$* , *JHEP* **06** (2016) 131 [[1604.01525](#)].
- [24] LHCb COLLABORATION, R. Aaij et al., *Measurement of the CKM angle  $\gamma$  using  $B^\pm \rightarrow DK^\pm$  with  $D \rightarrow K_S^0 \pi^+ \pi^-$ ,  $K_S^0 K^+ K^-$  decays*, *JHEP* **2018** (2018) 176 [[1806.01202](#)].
- [25] LHCb COLLABORATION, *Physics case for an LHCb Upgrade II*, [1808.08865](#).
- [26] BELLE II COLLABORATION, *The Belle II Physics book*, [1808.10567](#).
- [27] Y. Grossman and M. Savastio, *Effects of  $K^0-\bar{K}^0$  mixing on determining  $\gamma$  from  $B^\pm \rightarrow DK^\pm$* , *JHEP* **03** (2014) 008 [[1311.3575](#)].
- [28] LHCb COLLABORATION, R. Aaij et al., *Measurement of CP asymmetry in  $D \rightarrow K^- K^+$  and  $D \rightarrow \pi \pi$  decays*, *JHEP* **2014** (2014) 41 [[1405.2797](#)].
- [29] A. Davis, L. Dufour, L. Dufour, F. Ferrari, S. Stahl, J. Van Tilburg et al., *Measurement of the instrumental asymmetry for  $K^- \pi^+$ -pairs at LHCb in Run 2*, Tech. Rep. LHCb-PUB-2018-004. CERN-LHCb-PUB-2018-004, CERN, Geneva, March, 2018.

- [30] A. Bondar, A. Poluektov and V. Vorobiev, *Charm mixing in a model-independent analysis of correlated  $D^0\bar{D}^0$  decays*, *Phys.Rev.* **D82** (2010) 034033 [[1004.2350](#)].
- [31] A. Bondar, A. Dolgov, A. Poluektov and V. Vorobiev, *Effect of direct CP violation in charm on  $\gamma$  extraction from  $B \rightarrow DK^\pm, D \rightarrow K_S^0\pi^+\pi^-$  Dalitz plot analysis*, *Eur. Phys. J.* **C73** (2013) 2476 [[1303.6305](#)].
- [32] CLEO COLLABORATION, J. Libby et al., *Model-independent determination of the strong-phase difference between  $D^0$  and  $\bar{D}^0 \rightarrow K_{S,L}^0 h^+ h^-$  ( $h = \pi, K$ ) and its impact on the measurement of the CKM angle  $\gamma/\phi_3$* , *Phys.Rev.* **D82** (2010) 112006 [[1010.2817](#)].
- [33] C. Thomas and G. Wilkinson, *Model-independent  $D^0 - \bar{D}^0$  mixing and CP violation studies with  $D^0 \rightarrow K_S^0\pi^+\pi^-$  and  $D^0 \rightarrow K_S^0 K^+ K^-$* , *JHEP* **10** (2012) 185 [[1209.0172](#)].
- [34] LHCb COLLABORATION, R. Aaij et al., *Near-threshold  $D\bar{D}$  spectroscopy and observation of a new charmonium state*, [1903.12240](#).
- [35] PARTICLE DATA GROUP, M. Tanabashi et al., *Review of particle physics*, *Phys. Rev. D* **98** (2018) 030001.
- [36] A. Pais and O. Piccioni, *Note on the Decay and Absorbtion of the  $\theta^0$* , *Phys. Rev.* **100** (1955) 1487.
- [37] M. L. Good, *Relation between Scattering and Absorbtion in the Pais-Piccioni Phenomenon*, *Phys. Rev.* **106** (1957) 591.
- [38] W. Fetscher et al., *Regeneration of arbitrary coherent neutral kaon states: A new method for measuring the  $K^0 - \bar{K}^0$  forward scattering amplitude*, *Z. Phys. C* **72** (1996) 543.
- [39] BABAR AND BELLE COLLABORATIONS, I. Adachi et al., *Measurement of  $\cos 2\beta$  in  $B^0 \rightarrow D^{(*)}h^0$  with  $D \rightarrow K_S^0\pi^+\pi^-$  decays by a combined time-dependent Dalitz plot analysis of BaBar and Belle data*, *Phys. Rev.* **D98** (2018) 112012 [[1804.06153](#)].
- [40] I. I. Y. Bigi and H. Yamamoto, *Interference between Cabibbo allowed and doubly forbidden transitions in  $D \rightarrow K_{S/L} + \pi$ 's decays*, *Phys. Lett.* **B349** (1995) 363 [[hep-ph/9502238](#)].
- [41] CLEO COLLABORATION, Q. He et al., *Comparison of  $D \rightarrow K_S^0\pi$  and  $D \rightarrow K_L^0\pi$  Decay Rates*, *Phys. Rev. Lett.* **100** (2008) 091801 [[0711.1463](#)].
- [42] Y. Grossman and Y. Nir, *CP violation in  $\tau^\pm \rightarrow \pi^\pm K_S^0\nu$  and  $D^\pm \rightarrow \pi^\pm K_S^0$ : the importance of  $K_S^0 - K_L^0$  interference*, *JHEP* **2012** (2012) 2 [[1110.3790](#)].
- [43] G. Cowan, D. Craik and M. Needham, *RapidSim: An application for the fast simulation of heavy-quark hadron decays*, *Computer Physics Communications* **214** (2017) 239 [[1612.07489](#)].
- [44] LHCb COLLABORATION, *LHCb VELO Upgrade Technical Design Report*, Tech. Rep. CERN-LHCC-2013-021. LHCb-TDR-013, November, 2013.
- [45] LHCb COLLABORATION, *LHCb PID Upgrade Technical Design Report*, Tech. Rep. CERN-LHCC-2013-022. LHCb-TDR-014, November, 2013.
- [46] A. Poluektov, *Unbinned model-independent measurements with coherent admixtures of multibody neutral d meson decays*, *Eur. Phys. J.* **C78** (2018) 121 [[1712.08326](#)].
- [47] D. J. Lange, *The EvtGen particle decay simulation package*, *Nucl. Instrum. Meth.* **A462** (2001) 152.
- [48] M. Kenzie, M. Martinelli and N. Tuning, *Estimating  $r_B^{D\pi}$  as an input to the determination of the CKM angle  $\gamma$* , *Phys. Rev. D* **94** (2016) 054021 [[1606.09129](#)].

- [49] P. K. Resmi, J. Libby, S. Malde and G. Wilkinson, *Quantum-correlated measurements of  $D \rightarrow K_S^0 \pi^+ \pi^- \pi^0$  decays and consequences for the determination of the CKM angle  $\gamma$* , *JHEP* **01** (2018) 082 [[1710.10086](https://arxiv.org/abs/1710.10086)].
- [50] LHCb COLLABORATION, *LHCb reoptimized detector design and performance: Technical Design Report*, Tech. Rep. CERN-LHCC-2003-030, LHCb-TDR-9, CERN, Geneva, 2003.
- [51] J. Gassner, M. Needham and O. Steinkamp, *Layout and Expected Performance of the LHCb TT Station*, Tech. Rep. LHCb-2003-140, CERN, Geneva, April, 2004.
- [52] BELLE, A. B. Kaliyar et al., *Measurements of branching fraction and direct  $cp$  asymmetry in  $B^\pm \rightarrow K_S^0 K_S^0 K^\pm$  and a search for  $B^\pm \rightarrow K_S^0 K_S^0 \pi^\pm$* , *Phys. Rev. D* **99** (2019) 031102.
- [53] H. Nakano, *Search for new physics by a time-dependent  $CP$  violation analysis of the decay  $B \rightarrow K_S^0 \eta \gamma$  using the Belle detector*, Ph.D. thesis, Tohoku University, Sendai, 2015. [<http://hdl.handle.net/10097/58814>].
- [54] A. Gsponer et al., *Precise Coherent  $K_S^0$  Regeneration Amplitudes for C, Al, Cu, Sn, and Pb Nuclei from 20 to 140 GeV/c and Their Interpretation*, *Phys. Rev. Lett.* **22** (1979) 13.
- [55] R. A. Briere and B. Winstein, *Determining the Phase of a Strong Scattering Amplitude from Its Momentum Dependence to Better Than  $1^\circ$ : The Example of Kaon Regeneration*, *Phys. Rev. Lett.* **75** (1995) 402.
- [56] B. R. Ko, E. Won, B. Golob and P. Pakhlov, *Effect of nuclear interactions of neutral kaons on  $CP$  asymmetry measurements*, *Phys. Rev. D* **84** (2011) 111501 [[1006.1938](https://arxiv.org/abs/1006.1938)].
- [57] LHCb COLLABORATION, *LHCb RICH1 Engineering Design Review Report*, Tech. Rep. LHCb-2004-121, CERN, Geneva, 2004.
- [58] Waleed Syed Ahmed and Steven Robertson, *Material Budget Studies for the Belle-II Detector*, BELLE2-MTHESIS-2017-012, Master's thesis, McGill University, Montreal, 2017.